JOURNAL OF PHYSICAL ORGANIC CHEMISTRY
J. Phys. Org. Chem. 2003; **16:** 675–681
Published online in Wiley InterScience (www.interscience.wiley.com). DOI: 10.1002/poc.667

Potential-controlled coordination of coumarin to an Au(210) electrode surface†

Anna Iannelli and Jacek Lipkowski*

Department of Chemistry and Biochemistry, University of Guelph, Guelph Ontario, N1G 2W1, Canada

Received 31 January 2003; revised 9 April 2003; accepted 10 April 2003

ABSTRACT: Adsorption of coumarin on an Au(210) single-crystal electrode was investigated using chronocoulometry and phase-sensitive a.c. voltammetry. The adsorption parameters, such as the relative Gibbs surface excess, the Gibbs energies of adsorption and the electrosorption valencies, were calculated. The results suggest that coumarin molecules assume a flat, π-bonded orientation on the Au(210) surface. The zero coverage Gibbs energy of adsorption at the potential of maximum adsorption is $-42\,\mathrm{kJ\,mol^{-1}}$, which is a value typical of chemisorption. The adsorption of coumarin on the Au(210) surface was compared with adsorption at the (111) and (100) planes of gold. Copyright © 2003 John Wiley & Sons, Ltd.

KEYWORDS: coumarin adsorption; gold single-crystal electrode; surface coordination; chronocoulometry

INTRODUCTION

This work constitutes part of a series devoted to the investigation of the coordination of organic compounds to metal electrode surfaces.[1,2] Here, we describe potential-controlled coordination of coumarin to the Au(210) electrode surface. Coumarin, also known as 2*H*-1-benzopyran-2-one, is a bicyclic molecule with two electronegative oxygen atoms situated in one of the aromatic rings. Coumarin is a valuable leveling agent used in electroplating and its most popular use is in semi-bright nickel plating which yields deposits that are semi-lustrous and can be easily polished to a mirror finish.[4–6] There has been significant interest in coumarin adsorption on a mercury electrode where potential controlled formation of a condensed film was observed.[7–12] Coumarin adsorption on Au(111)[1,13] and Au(100)[14,15] gold electrode surfaces has been investigated recently.

The object of this work was to complement recent studies of coumarin adsorption on gold single-crystal surfaces[13–15] in order to provide a more complete description of the effect of surface crystallography on the coordination of this molecule to a Au electrode surface. Low-index and hence the most densely packed and the least reactive single-crystal surfaces were used in previous studies. Here, we employed the Au(210) plane, which is the least densely packed single-crystal plane. Figure 1 shows the hard-ball model of this surface. It has a very open structure and the highest density of broken bonds. It is the most reactive gold surface. The stability of the Au(210) surface in vacuum and at the metal–solution interface has been investigated[16,17] and these studies demonstrated that it does not reconstruct and that its nominal crystallography is preserved at the metal–solution interface. In this work, we determined Gibbs excesses and Gibbs energies for coumarin adsorption at the Au(210) surface–electrolyte interface and compared these data with those determined earlier for Au(111) and Au(100) surfaces.

EXPERIMENTAL

An Au(210) single crystal (99.99% purity) was grown in our laboratory. Before each experiment, the electrode was flame annealed. Contact between the gold surface and the electrolyte was made by using a hanging meniscus technique.[18] Experiments were performed in a cell equipped with a gold electrode, a gold foil counter electrode and an external saturated calomel electrode (SCE) connected to the cell with a Luggin capillary. The supporting electrolyte was 0.1 M $KClO_4$. The $KClO_4$ (ACS Certified, Fisher) was purified as described.[19] Coumarin (Aldrich, 99+%) was used without further purification. All solutions were prepared using Milli-Q-purified water (Millipore) with a resistivity 18 MΩ cm. Argon was used to remove oxygen from the investigated solution. All experiments were carried out at $25 \pm 1\,^{\circ}\mathrm{C}$. The electrochemical experiments were performed using a PAR Model 173 potentiostat controlled by a computer. The data were acquired via a plug-in acquisition board (RC Electronics Model IS-16). Custom software was

**Correspondence to:* J. Lipkowski, Department of Chemistry and Biochemistry, University of Guelph, Guelph, Ontario, N1G 2W1, Canada.
E-mail: Lipkowski@chembio.uoguelph.ca
†Dedicated to Professor T. M. Krygowski in recognition of his outstanding contribution to physical organic chemistry.
Contract/grant sponsor: NSERC.

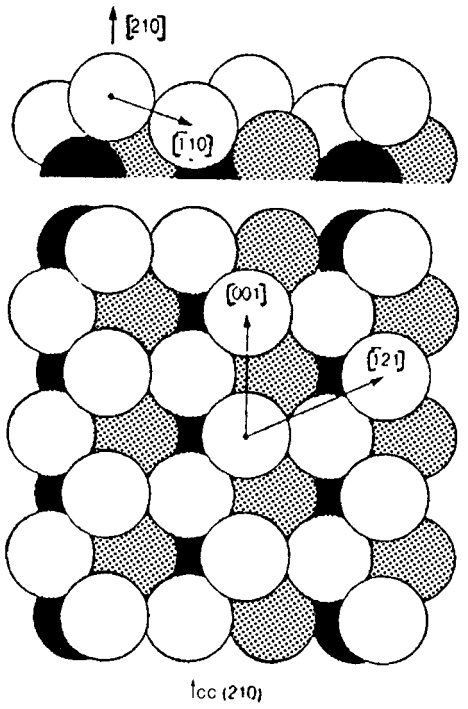

Figure 1. Hard-ball model of the Au(210) surface. Top, side view; bottom, top view. With permission from reference 22

used to perform the chronocoulometric experiments. A PAR Model 5204 two-phase lock-in amplifier was used for differential capacity measurements.

RESULTS

Differential capacity

The adsorption of coumarin on Au(210) was initially characterized by recording differential capacity curves. The differential capacities were determined using a slow $5\,\mathrm{mV\,s^{-1}}$ potential sweep in the direction of positive potentials and 25 Hz r.m.s. a.c. perturbation. The capacities were calculated from the measured out-of-phase and in-phase components of the a.c. signal assuming a simple *RC* circuit. To enhance mass transport towards the electrode, the solutions were stirred during the data acquisition. Figure 2 shows the differential capacity curves determined for the pure supporting electrolyte and a series of coumarin solutions. It should be emphasized that the capacities, determined at a single frequency of 25 Hz, do not represent the state of adsorption equilibrium. They are shown here to characterize the interface qualitatively.

The curve for the supporting electrolyte displays a well-defined diffuse layer minimum. The potential of zero charge (pzc) determined from the position of this minimum is -0.095 V (vs SCE), in good agreement with the value of -0.08 ± 0.01 V determined by Hamelin for $LiClO_4$ solution.[20]

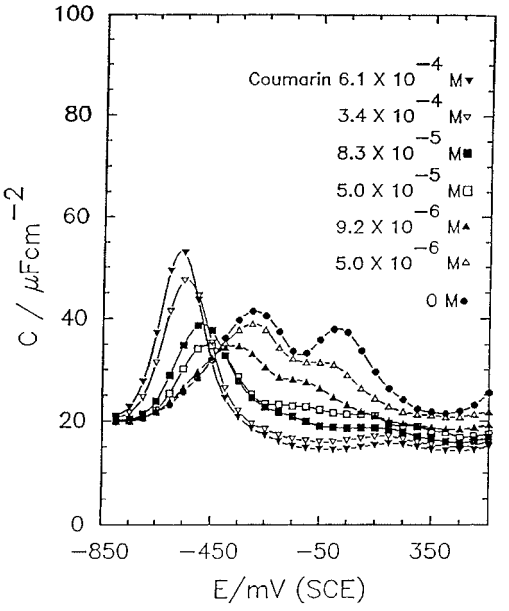

Figure 2. Differential capacity curves for the Au(210) surface for 0.1 M $KClO_4$ solutions without and with various coumarin concentrations

When coumarin is added to the solution, the capacity decreases at potentials close to the pzc. When the coumarin concentration is higher than 5×10^{-5} M, a characteristic adsorption/desorption peak appears on the capacity curves. At potentials more negative than -0.8 V (vs SCE), the capacity curves recorded in the presence of coumarin merge with the curve for the supporting electrolyte. This behavior indicates that coumarin is desorbed from the electrode surface at these negative potentials.

Charge densities

Potential step experiments were performed to determine quantitative data for coumarin adsorption on the Au(210) surface. The electrode was initially held at an initial potential E_i at which coumarin adsorption took place for a period of $\sim$3 min while the solution was stirred vigorously. The stirring was interrupted and the solution was allowed to calm down during an additional waiting period of 1 min. The potential was then stepped to the final potential E_j of -0.8 V (vs SCE), at which coumarin totally desorbs from the electrode surface. The current transient corresponding to the charging of the interface was recorded and integrated to give the relative charge density $\Delta\sigma_M$ as described.[19] Using the value of the pzc, the absolute charge density at the initial potential was calculated using the procedure described previously.[1,19]

Figure 3 shows the charge density curves determined for the Au(210) electrode in the presence and absence of coumarin. The curves in the presence of coumarin intersect the curve for the supporting electrolyte at $E \approx -0.050$ V (vs SCE), indicating that this is the

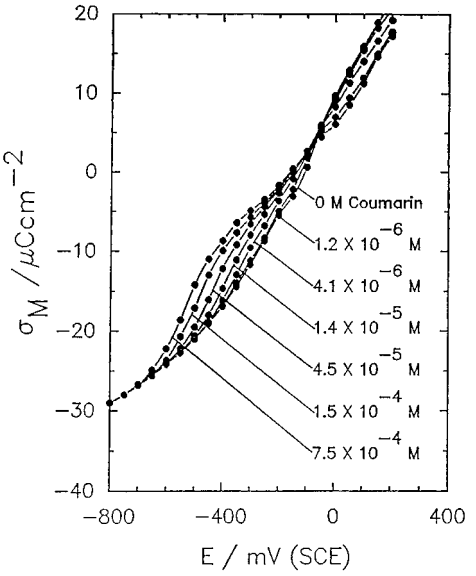

Figure 3. Charge density versus electrode potential plots determined for 0.1 M $KClO_4$ solutions without and with various coumarin concentrations

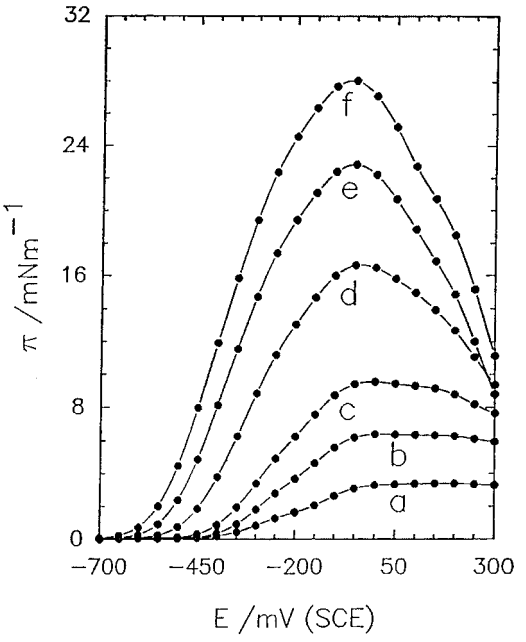

Figure 4. Film pressure at constant potential plotted versus the electrode potential for 0.1 M $KClO_4$ solutions of varying coumarin concentration: (a) 1.9×10^{-6}; (b) 4.1×10^{-6}; (c) 9.2×10^{-6}; (d) 4.5×10^{-6}; (e) 1.5×10^{-6}; (f) 5.0×10^{-6} M

potential of the maximum adsorption (E_{max}). They merge with the curve for the supporting electrolyte at $E < -0.7$ V (vs SCE), indicating total desorption at these negative potentials. The charge density curves constitute the basic set of experimental data from which the Gibbs excess and Gibbs energy of adsorption will be calculated.

Gibbs excesses

The charge density curves were integrated and the film pressure of adsorbed coumarin at constant potential $\pi = \gamma_{c=0} - \gamma_c$ ($\gamma_{c=0}$ and γ_c are the surface energies in the absence and presence of coumarin in the solution) was calculated using the procedure described previously.[1,19] The film pressures are plotted against potential in Fig. 4. The curves are bell-shaped. Their maximum shifts slightly from ~0 to ~−0.05 V (vs SCE) from the lowest to the highest coumarin concentration.

In addition, the Parsons function $\xi = \gamma + \sigma_M E$ was calculated and the film pressure at constant charge, $\phi = \xi_{c=0} - \xi_c$, was determined as a function of the charge density. The film pressures at constant charge are plotted against the charge density in Fig. 5. The curves are also bell-shaped with the maximum shifting with the coumarin concentration from ~15 to ~7 μC cm^{-2}.

The relative Gibbs excess of coumarin was then calculated by differentiation of the film pressures with respect to the logarithm of the bulk coumarin concentration at constant potential or at constant charge:[1]

$$\Gamma = \left(\frac{\partial \pi}{RT \partial \ln c}\right)_E \qquad (1)$$

or

$$\Gamma = \left(\frac{\partial \phi}{RT \partial \ln c}\right)_{\sigma_M} \qquad (2)$$

The Gibbs excesses calculated with the help of these expressions are plotted in Figs 6(a) and (b), respectively. These graphs are three-dimensional, to show how the

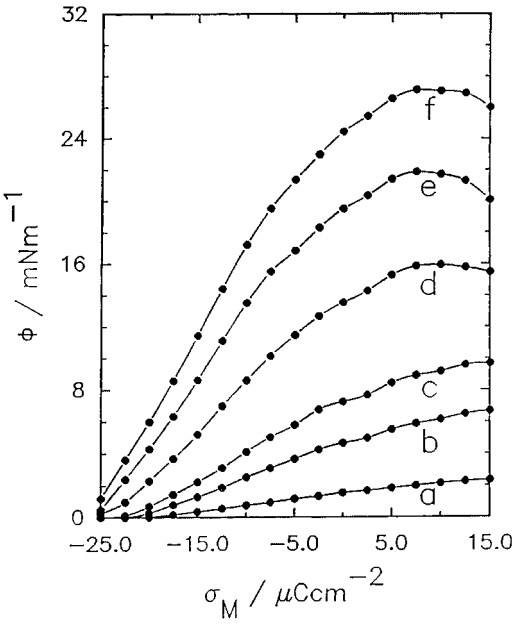

Figure 5. Film pressure at constant charge plotted versus charge density for 0.1 M $KClO_4$ solutions of varying coumarin concentration: (a) 1.9×10^{-6}; (b) 4.1×10^{-6}; (c) 9.2×10^{-6}; (d) 4.5×10^{-6}; (e) 1.5×10^{-6}; (f) 5.0×10^{-6} M

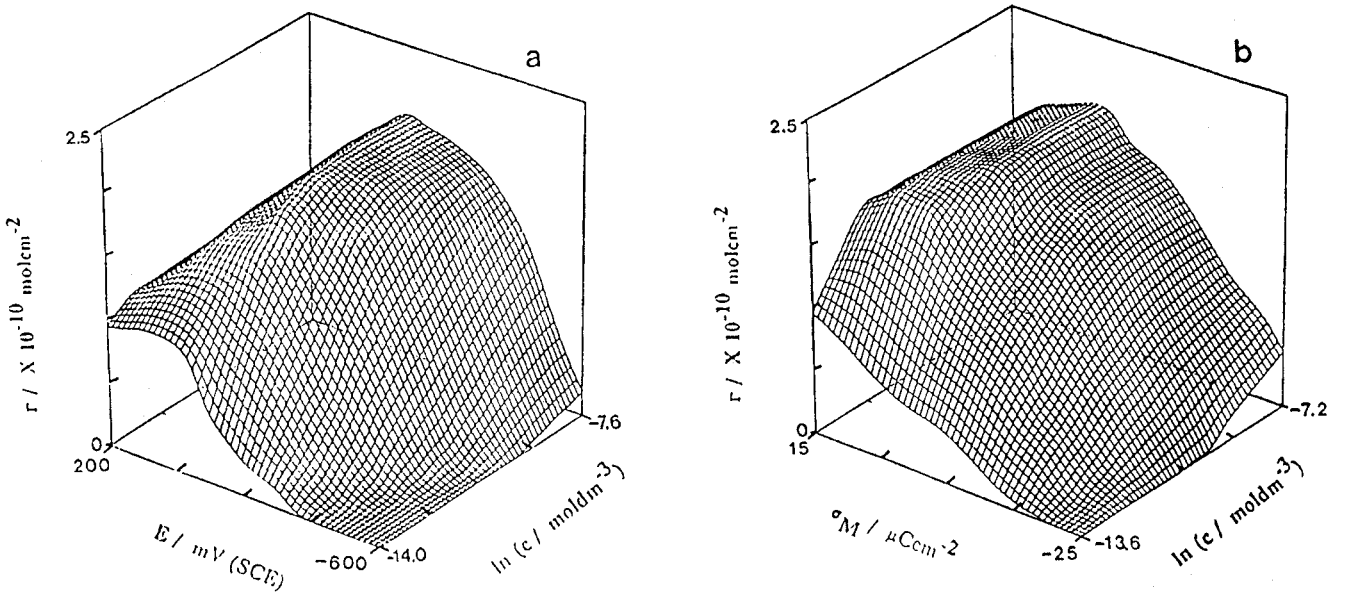

Figure 6. Three-dimensional graphs representing isotherms for adsorption of coumarin on the Au(210) surface with (a) potential and (b) charge density as the independent electrical variable

Gibbs excess depends on both the bulk concentration and the electrical variable. The Gibbs excesses are plotted on the vertical axis. The electrical variable [E in Fig. 6(a) and σ_M in Fig. 6(b)] and the logarithm of the bulk coumarin concentration are plotted at the axes located in the basal plane. At a constant electrical variable, the dependence of Γ on the logarithm of the bulk coumarin concentration has a sigmoidal (Langmurian) shape. At a constant bulk concentration, the change of Γ with the electrical variable displays a maximum. The values of E_{max} and $\sigma_{M,max}$ agree well with the values of the potential and charge of maximum adsorption observed earlier on the film pressure plots. The maximum value of the Gibbs excess Γ_{max} is 2×10^{-10} mol cm^2.

Gibbs energy of adsorption

The free energy of adsorption (ΔG_0) is usually determined from a fit of the experimental surface excess data to an equation of a particular adsorption isotherm. The choice of the isotherm used in the fit is usually arbitrary. However, in the limit of zero coverage, most of the common isotherms simplify to the Henry isotherm:[1]

$$\pi(\text{or } \phi) = RT\Gamma_{max}\beta c/55.5 \qquad (3)$$

where β is the adsorption equilibrium constant and is related to the standard Gibbs energy of adsorption through the equation $\Delta G_0 = -RT\ln\beta$. The equilibrium constant may be determined from the initial slopes of the film pressure versus the bulk concentration plots using the equation[1]

$$\beta = (\partial\pi/\partial X_b)_{X_b \to 0}/RT\Gamma_{max} \qquad (4)$$

where $X_b = c/55.5$ is the mole fraction of coumarin in the bulk solution.

The Gibbs energies of adsorption determined using this procedure are plotted against the electrode potential and charge density in Figs 7 and 8, respectively. Independently, the Gibbs energies were determined by fitting the Gibbs excess data to the equation of the Langmuir isotherm:

$$\frac{1}{\Gamma} = \frac{1}{\Gamma_{max}\beta c} + \frac{1}{\Gamma_{max}} \qquad (5)$$

Consistent with Eqn (5), linear relations were obtained when $1/\Gamma$ was plotted against $1/c$. The slope of these lines

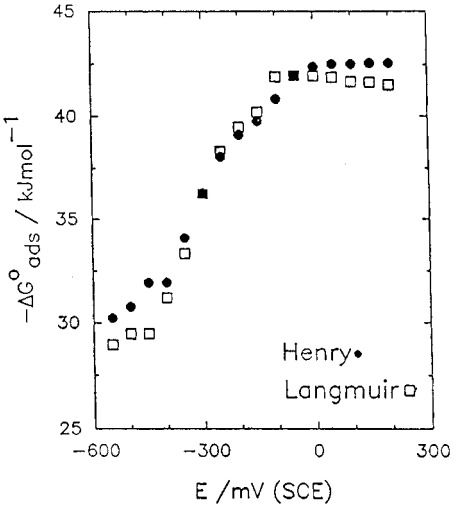

Figure 7. Zero coverage Gibbs energy of adsorption plotted versus the electrode potential, determined from Henry's law (solid symbols) and a fit to the Langmuir isotherm (open symbols)

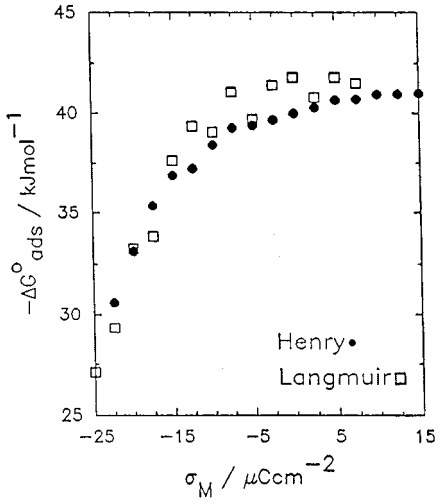

Figure 8. Zero coverage Gibbs energy of adsorption plotted versus charge density, determined from Henry's law (solid symbols) and a fit to the Langmuir isotherm (open symbols)

corresponded to $1/(\Gamma_{max}\beta)$ and the intercept to $1/\Gamma_{max}$. The equilibrium constant β is then equal to the ratio of the intercept to the slope. The Gibbs energies determined by fitting the data to the equation of the Langmuir isotherm are also plotted in Figs 7 and 8. The differences between the Gibbs energies determined by using the Henry isotherm and fitting the Gibbs excess data to the Langmuir isotherm are very small. The Langmuir isotherm is derived assuming that the surface layer behaves as a perfect solution with energy of lateral interactions equal to zero.[1] The agreement between the Gibbs energies determined from the Henry's law and from the Langmuir isotherm indicates that the energy of lateral interaction between adsorbed coumarin molecules is negligible. The Gibbs energy plots in Figs 7 and 8 displays a quasi-parabolic dependence on the electrical variable. This is a typical behavior for adsorption of organic molecules on metal electrodes.[1]

The determination of the Gibbs excesses and Gibbs energies of adsorption involved at least one integration and one differentiation step. It is useful to employ the so-called cross-differential equations to verify whether no major errors were made in the numerical data processing. Differentiation of the electrocapillary equation gives the expression for electrosorption valency l (IUPAC recommends term formal charge transfer number at a constant potential):[1]

$$l = \frac{1}{F}\left(\frac{\partial \Delta G_0}{\partial E}\right)_{\Gamma} = -\frac{1}{F}\left(\frac{\partial \sigma_M}{\partial \Gamma}\right)_{E} \qquad (6)$$

Equation (6) shows that a derivative of the Gibbs energy at zero coverage should be equal to the slope of the charge density versus Gibbs excess plot at a constant potential.

Figure 9 shows charge density plotted versus Gibbs excess for selected electrode potentials. The initial slopes

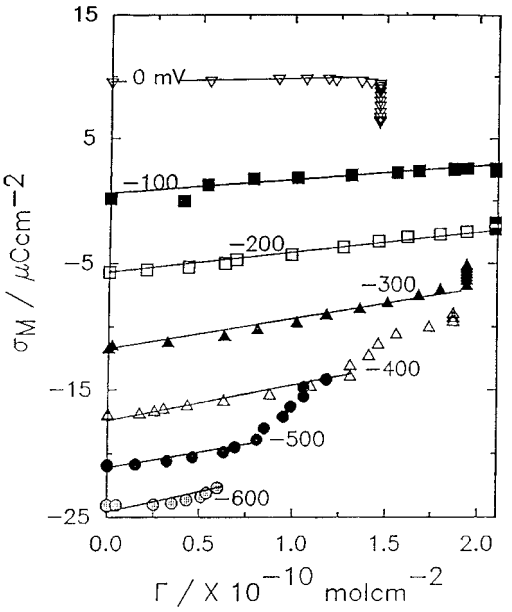

Figure 9. Plots of charge density versus the surface excess of coumarin for different values of the electrode potential as indicated (in mV vs SCE). The straight lines were drawn through points corresponding to low values of the Gibbs excess

of these plots give the electrosorption valency l at zero coverage. The experimental points in Fig. 10 show the dependence of the electrosorption valency on the electrode potential. The solid line in Fig. 10 was determined by fitting the Gibbs energy plot (determined from Henry's

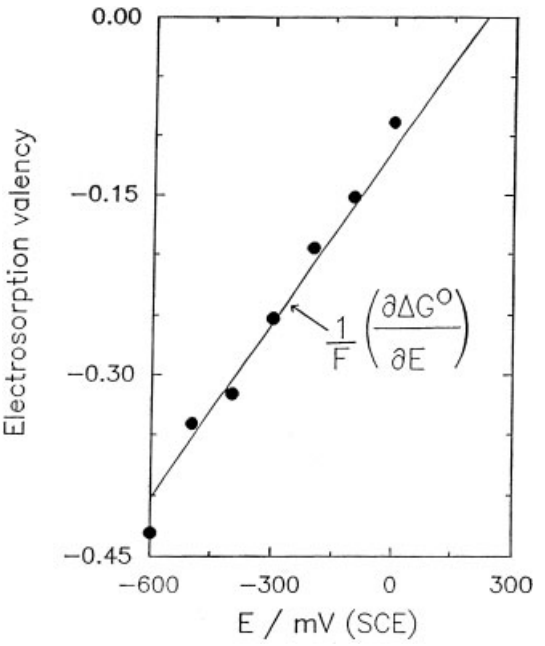

Figure 10. Electrosorption valency plotted versus the electrode potential. The points correspond to the data obtained from the initial sections of the charge density versus the Gibbs excess plots in Fig. 9. The line corresponds to the first derivative of a second-order polynomial used to fit the Gibbs excess curve for Henry's law in Fig. 7

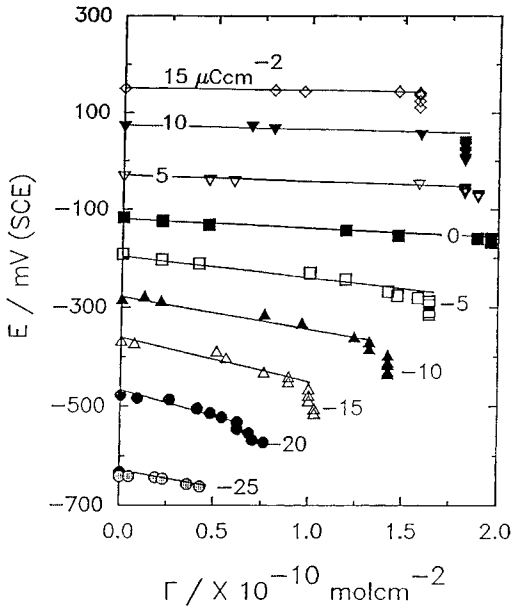

Figure 11. Plots of the electrode potential versus the surface excess of coumarin for different values of charge densities as indicated. The straight lines were drawn through points corresponding to low values of the Gibbs excess

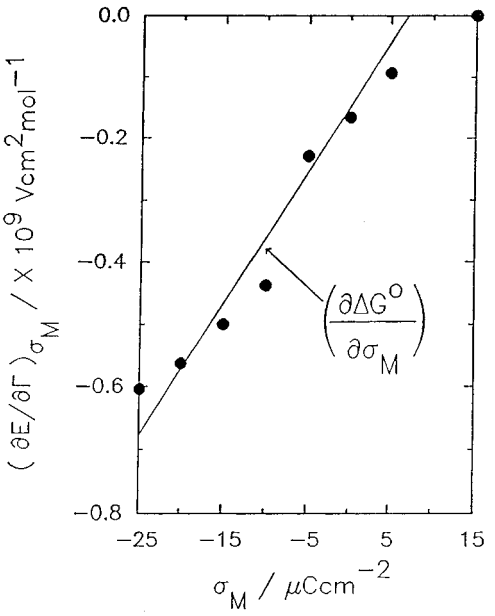

Figure 12. Dependence of $(\partial E/\partial\Gamma)_{\sigma_M}$ on the charge density. The points were calculated from initial slopes of the plots in Fig. 11. The solid line corresponds to the first dervative of a second-order polynomial used to fit the Gibbs energy curve (determined from Henry's law) in Fig. 8

law) in Fig. 7 to a second-order polynomial and differentiating this polynomial. The agreement between the electrosorption valencies calculated by the two methods is very good. This shows that no major errors were made in the numerical data processing. Consistent with Eqn (6), the linear dependence of the formal charge transfer on potential is consistent with the parabolic dependence of the Gibbs energy on E observed in Figs 7 and 8.

The absence of errors in the analysis carried out at constant charge can be verified using another cross-differential equation:[1]

$$\left(\frac{\partial E}{\partial \Gamma}\right)_{\sigma_M} = \left(\frac{\partial \Delta G_0}{\partial \sigma_M}\right)_{\Gamma} \tag{7}$$

In this case, the initial slopes of E versus Γ plots at selected values of σ_M should be equal to the derivative of ΔG_0 versus σ_M curve. Plots of the electrode potential versus the Gibbs excess at constant charge densities are shown in Fig. 11. The initial sections of these plots are linear. Their slopes are plotted against charge density in Fig. 12. The points show $(\partial E/\partial\Gamma)_{\sigma_M}$ values. The line is the first derivative of the second-order polynomial fitted to the Gibbs energy curve (determined from Henry's law) shown in Fig. 8. The agreement between the data calculated using different numerical procedures is very good and shows that the data processing did not introduce significant errors.

DISCUSSION

We have determined Gibbs excesses and Gibbs energies for coumarin adsorption on the Au(210) surface. The results show that both Gibbs excess and Gibbs energy display a quadratic dependence on the electrical variable (potential or charge). The adsorption of coumarin is described well by a Langmuir isotherm and this feature suggests that the lateral interaction energy for molecules adsorbed at the interface is negligible. Table 1 compares adsorption parameters determined for coumarin adsorption on the Au(210) surface with the data determined for the Au(111)[13] and the Au(100) plane.[15,21] The data in Table 1 show that coumarin adsorption is essentially independent of the crystallographic orientation and hence is insensitive to structure. The value of the maximum

Table 1. Summary of adsorption parameters for coumarin adsorption on Au(*hkl*) electrodes

Electrode	E_{pzc} (mV vs SCE)	Γ_{max} ($\times 10^{10}$) (mol cm^{-2})	σ_{max} ($\times 10^{6}$) (μC cm^{-2})	$\Delta G_{0,max}$ (kJ mol^{-1})	$E_{max} - E_{pzc}$	Ref.
Au(210)	−95	2.0	∼5	−42	25	This work
Au(111)	+290	2.1	∼5	−42	60	13
Au(100)	+200	2.7	∼2	−40	∼20	15, 21
Hg	−450	2.9				10

Gibbs excess close to 2×10^{-10} mol cm^{-2} suggest that coumarin assumes a flat π-bonded orientation at all three single-crystal surfaces of gold when the bulk coumarin concentration is lower than 1 mM.

The small values of $\sigma_{M,max}$ and E_{max} suggest that the component of the permanent dipole moment in the direction normal to the surface is small for adsorbed molecules. An isolated coumarin molecule has a large permanent dipole moment of 4.5 D oriented in the plane of the molecule.[10] Therefore, the small values of $\sigma_{M,max}$ and E_{max} are consistent with the flat surface orientation. A similar orientation was observed earlier for coumarin adsorbed at a mercury electrode at positive potentials and low bulk coumarin concentration.[10] However, the small changes of $\sigma_{M,max}$ and E_{max} with the bulk coumarin concentration suggest that the tilt angle of adsorbed molecules may change somewhat with coverage. In the future, we will perform *in situ* infrared reflection absorption spectroscopic experiments to determine the tilt angle for adsorbed coumarin.

The independence of the Gibbs energy of coumarin adsorption of the crystallographic orientation is an unexpected result. Adsorption at a metal–solution interface is a solvent substitution process. When one organic molecule adsorbs at the surface, n water molecues are displaced into the bulk. This is described by the equation

$$A_b + nW_s = A_s + nW_b \quad (8)$$

where A represents an organic molecule and W water and the subscripts b and s represent bulk and surface, respectively. Thus, the free energy of adsorption is determined by the difference between the Gibbs energies of the organic molecule and n water molecules at the surface and in the bulk, respectively:

$$\Delta G_0 = \left(G_A^s - nG_W^s\right) - \left(G_A^b - nG_W^b\right) \quad (9)$$

The second term is surface independent. Therefore, the observed independence of ΔG_0 on the crystallographic orientation indicates that the changes of G_A^s and nG_W^s are of comparable magnitude and cancel each other.

The case of coumarin adsorption is unique and distinctly different from the case of weak physisorption of an aliphatic molecule such as diethyl ether[23] or chemisorption of an aromatic base such as pyridine.[1,24] For adsorption of diethyl ether on Au(*hkl*),[23] the Gibbs energy of adsorption becomes more positive on going from a more densely packed Au(111) to a more open Au(110) single-crystal face. It is improbable that G_A^s and nG_W^s become more positive when the gold surface is more open and hence more reactive. For this aliphatic molecule, the observed change of ΔG_0 indicates that the energy of the water–gold interaction increases on moving from a densely packed to a more open surface, making the nG_W^s term more negative.

For pyridine chemisorption on Au(*hkl*), the opposite trend is observed. The Gibbs energy of adsorption becomes more negative on moving from an Au(111) to an Au(210) surface.[1,24] Here, the energy of the gold–pyridine interaction changes more than the energy of the gold–water interaction and the change in the G_A^s term determines how the crystallographic orientation of the surface affects ΔG_0. We conclude that the case of coumarin adsorption on gold surfaces is intermediate between physisorption and chemisorption.

Acknowledgements

This work was supported by an NSERC research grant. J. L. acknowledges CFI for a Canada Research Chair award.

REFERENCES

1. Lipkowski J, Stolberg L. In *Adsorption of Molecules at Metal Electrodes*, Lipkowski J, Ross PN (eds). Wiley-VCH: New York, 1992; 171–238.
2. Lipkowski J, Stolberg L, Yang D-F, Pettinger B, Mirwald S, Henglein F, Kolb DM. *Electrochimi. Acta* 1994; **39**: 1057–1065.
3. Lipkowski J, Szymanski G, Chen A, Burgess I, Bizzotto D, Cai X, Hoon-Khoshla M, Jeffrey C. In *Metal–Ligand Interaction in Chemistry, Physics and Biology*, Rousso N, Salahub D (eds). NATO ASI Series. Kluwer: Dordrecht, 2000; 155–181.
4. Macheras J, Vouros D, Kollia C, Spyrellis N. *Trans. Inst. Met. Finish.* 1996; **4**: 55–58.
5. Cheng CC, West AC. *J. Electrochem. Soc.* 1997; **144**: 3050–3056.
6. Madore C, Landolt D. *J. Electrochem. Soc.* 1996; **143**: 3936–3943.
7. Thomas FG, Buess-Herman C, Gierst L. *J. Electroanal. Chem.* 1986; **214**: 597–613.
8. Bond AM, Thomas FG. *Langmuir* 1988; **4**: 341–345.
9. Srinivasan R, De Levie R. *J. Electroanal. Chem.* 1988; **249**: 321–326.
10. Partridge LK, Tansley AC, Porter AS. *Electrochim. Acta* 1966; **11**: 517–526.
11. Freymann M, Poelman M, Buess-Herman C. *Isr. J. Chem.* 1997; **37**: 241–246.
12. Damaskin BB, Baturina OA. *Russi. J. Electrochem.* 2002; **38**: 1141–1147.
13. Ianneli A, Richer J, Stolberg L, Lipkowski J. *Plating Surf. Finish.* 1990; **77**: 47–52.
14. Skoluda P, Hamm UW, Kolb DM. *J. Electroanal. Chem.* 1993; **354**: 289–294.
15. Hoelzle MH, Kolb DM. *Ber. Bunsen-Ges. Phys. Chem.* 1994; **98**: 330–335.
16. Lecoeur J, Bellier JP, Koehler C. *Electrochim. Acta* 1990; **35**: 1383–1392.
17. Sun SG, Yang DF, Wu SJ, Ociepa J, Lipkowski J. *J. Electroanal. Chem.* 1993; **349**: 211–222.
18. Dickertmann D, Schultze JW, Koppitz FD. *Electrochim. Acta* 1976; **21**: 967–971.
19. Richer J, Lipkowski J. *J. Electrochem. Soc.* 1986; **133**: 121–128.
20. Hamelin A. *J. Electroanal. Chem.* 1982; **138**: 395–400.
21. Hoelzle MH. PhD Thesis, University of Ulm, 1995; 58–68.
22. Maclaren JM, Pendry JB, Rous PJ, Saldin DK. *Surface Crystallographic Information Service. A Handbook of Surface Structutres*. Reidel: Boston, 1987.
23. Lipkowski J, Nguyen Van Huong C, Hinnen C, Parsons R, Chevalet J. *J. Electroanal. Chem.* 1983; **143**: 375–396.
24. Yang DF, Stolberg L, Lipkowski J, Irish DE. *J. Electroanal. Chem.* 1992; **329**: 259–278.